# Direct Molecular Dynamics Simulation of Flow Down a Chemical Potential Gradient in a Slit-Shaped Micropore

Roger F. Cracknell,[1] David Nicholson,[1,*] and Nicholas Quirke[2,*]

[1]*Department of Chemistry, Imperial College of Science, Technology and Medicine, London, SW7 2AY, United Kingdom*
[2]*European Centre for Computational Science and Technology, BIOSYM Technologies Sarl, Parc Club Orsay Université, 20 rue Jean Rostand, 91893 Orsay, France*

(Received 19 September 1994)

A novel nonequilibrium molecular dynamics simulation technique has been developed whereby the flux of particles, flowing between explicitly defined regions of different constant chemical potential, is measured directly by counting particles. The method uses both stochastic and dynamic steps. A linear relationship between flux and concentration gradient (Fick's law) is found for methane in a carbonaceous slit micropore with a diffuse wall condition. Diffusion coefficients thereby calculated are larger than transport diffusivities from equilibrium simulations using Darken's rule.

PACS numbers: 47.55.Mh, 05.60.+w, 61.20.Ja, 66.20.+d

Both the Onsager and Stefan-Maxwell formulations of irreversible thermodynamics recognize that the gradient of chemical potential is the driving force for isothermal mass transport [1] and that the flux can be identified as the sum of a cooperative viscous and a purely diffusive component [2]. Molecular dynamics simulations of cooperative viscous (Hagen-Poiseuille) flow [3–5] in pores have been carried out by giving each particle in the simulation an identical force in order to induce flow, with temperature rescaling to remove the heat artificially introduced in the system by the force. The magnitude of the force is unrealistically large, typically many orders of magnitude greater than gravity. Because of the constant particle density along the flow direction, these simulations give limited information about diffusive properties of the system, and calculations of viscosity (from Poiseuille's equation) make the questionable assumption that continuum hydrodynamics still applies to highly confined fluids [6].

Self-diffusion coefficients can be calculated using standard equilibrium molecular dynamics (EMD) either from the time evolution of the mean squared displacement (Einstein relation) or from an integral over the velocity autocorrelation function (Green-Kubo relation) [7]. The self-diffusion coefficient, multiplied by the so-called Darken factor, $d\ln f/d\ln\rho$ (where $f$ is the bulk gas fugacity, $\rho$ is the density of fluid in the pore), gives a value for the "transport diffusion coefficient" [8]. However, this approach ignores viscous cooperative effects and also requires that the system remains close to equilibrium, since the diffusion coefficients in EMD are calculated from equilibrium fluctuations.

The objective of this work was to develop a viable nonequilibrium molecular dynamics (NEMD) scheme which can simultaneously simulate both the diffusive and viscous components of the molecular transport and can operate arbitrarily far from equilibrium. Maginn, Bell, and Theodorou developed two NEMD schemes for transport diffusion restricted to the linear response regime [9]. In our simulation scheme shown in Fig. 1, the source and sink regions are maintained at different chemical potentials. Particles flow down the chemical potential gradient (in the $x$ direction) and the flux is measured by counting particles flowing between the regions of controlled chemical potential, thereby providing a direct realization of a Thévenin ensemble [10]. These conditions relate directly to those prevailing in many applications of, and experiments on, porous materials, in which flux is driven by a chemical potential gradient [8]. Our approach has certain similarities to that of Sun and Ebner [11], who maintained their source region at constant density by compressing the particles in this region into a new, smaller volume and inserting additional particles into the empty part of the old volume, the sink region being held at zero density by deleting any particles entering it. Our method for maintaining the chemical potentials in the end regions uses stochastic particle creation and deletion trials according to the prescription of grand canonical Monte Carlo (GCMC) [7]. The viability of such a synthesis of the elements of GCMC and MD into "Grand Canonical Molecular Dynamics" has been demonstrated by Cielinski and Quirke [12] and by later workers [13,14]. Heffelfinger and van Swol have developed a method of this type,

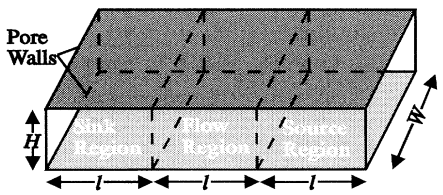


FIG. 1. NEMD simulation scheme. Chemical potentials are constant in the sink and source regions, where stochastic (GCMC) creation and destruction occur (see text). A dynamic simulation is implemented in the flow region.

0031-9007/95/74(13)/2463(4)$06.00  

but without a chemical potential gradient, for directly simulating tracer diffusion [15].

The dynamic part of the simulation uses a Verlet leapfrog algorithm [7] with a time step of 3.7 fs. The stochastic part of the simulation employs the usual GCMC prescription [7] for creation and destruction trials in each control region separately. Creations are accepted with probability

$$P_{\mathrm{acc}}^{\mathrm{cr}} = \min\left[1, \frac{N+1}{zV}\exp(-\beta\Delta E)\right], \quad (1)$$

where $z = \exp(\beta\mu)/\Lambda^3$ is the absolute activity at temperature $kT = 1/\beta$, $\mu$ is the chemical potential, and $\Lambda$ is the de Broglie wavelength,

$$\Lambda = (\beta h^2/2\pi m)^{1/2}. \quad (2)$$

The volume $V$ and number of particles $N$ refer to the control volumes in question [12], not to the whole system. When a creation is accepted, the particle is given a velocity, selected from a Maxwell-Boltzmann distribution corresponding to the simulation temperature. To this is added a value for the streaming velocity taken from the simulation (see below). Destructions from a given control region are accepted with probability

$$P_{\mathrm{acc}}^{\mathrm{dest}} = \min\left[1, \frac{zV}{N}\exp(-\beta\Delta E)\right]. \quad (3)$$

Microscopic reversibility requires that the number of creation attempts be equal to the number of destruction attempts in each region. Periodic boundary conditions [7] are applied in the direction normal to the flow. In the direction parallel to the flow, particles crossing the end of the box leave the simulation. In preliminary investigations of possible schemes, we tried a method with periodic boundaries in the flow direction and an extra flow region spanning a periodic boundary. This necessitated a zero streaming velocity in the two control regions and caused a spurious discontinuity in velocity at the boundaries between regions. Because particles can flow out of the system into oblivion, a high ratio of stochastic to dynamical moves is required in order to maintain the concentration corresponding to the chemical potential in the control region (the "correct" relationship between chemical potential and concentration is established in separate equilibrium GCMC simulations [7]). Stochastic:dynamic ratios of between 20:1 and 110:1 were used for the state conditions we studied.

The streaming velocity added to the molecular velocities of newly created particles is calculated by taking a value for the flux and dividing it by the concentration in the control regions [1]. However, since flux is the object of the simulation, it is necessary to give the particles a suitable initial streaming velocity, and to update this from calculated fluxes as the simulation proceeds. The system was prone to chaotic instabilities, depending on the way that measured streaming velocities were fed back. A coarse grained feedback (flux averaged over the previous 1000 time steps) was found to be essential in order to avoid the flux diverging to infinity.

It is vital to maintain the system at the correct constant temperature to ensure that transport of matter is due to chemical potential gradients and not to thermal gradients [1,2]. To implement this the simulation box was divided into 20 sub-boxes in the flow direction and the kinetic energy *in each sub-box* was kept constant using a Gaussian constraint in the leapfrog scheme [16]. The streaming velocity does not contribute to the temperature and must be subtracted from the $x$ component of the velocity vectors prior to thermostating, but as discussed above this quantity is not known accurately during the simulation. For situations where the streaming velocity is much smaller than the molecular velocity, subtracting a coarse grained average streaming velocity caused negligible errors. Conversely, if the streaming velocity is comparable to the molecular velocity, it is possible only to thermostat in the coordinate directions normal to the flow, the temperature in the flow direction being controlled by molecular relaxation among the degrees of freedom.

We examined both specular and diffuse reflection wall conditions [8]. The diffuse condition was implemented by reselecting the velocities parallel to the wall from a Maxwell-Boltzmann distribution after collision (this also augments the temperature control), leaving the dynamics of the normal component unchanged. The particle was deemed to have hit the wall when (i) it was in the repulsive region of the potential, and (ii) the velocity normal to the wall reversed its sign between time steps. A fuller discussion of the implementation of the diffuse condition for a continuous wall potential is given elsewhere [17].

The fluid was modeled as Lennard-Jones particles, with pair interactions between particles separated by $r_{ij}$ given by

$$u_{ij} = -4\epsilon\left[\left(\frac{\sigma}{r_{ij}}\right)^6 - \left(\frac{\sigma}{r_{ij}}\right)^{12}\right]. \quad (4)$$

Methane parameters were used: $\sigma = 0.381$ nm and $\varepsilon/k = 148.1$ K [17]. The pair interactions were truncated at $r_{ij} = 5\sigma$. Long-range corrections were not applied. The interaction energy between a fluid particle and an individual pore wall (modeled as a graphite surface) was given by the 10-4-3 potential of Steele [18],

$$u_{sf}(z) = 2\pi\rho_s\epsilon_{sf}\sigma_{sf}^2\Delta\left\{\frac{2}{5}\left(\frac{\sigma_{sf}}{z}\right)^{10} - \left(\frac{\sigma_{sf}}{z}\right)^4 - \frac{\sigma_{sf}^4}{3\Delta(0.61\Delta + z)^3}\right\}, \quad (5)$$

where $\Delta$ is the separation between graphite layers ($= 0.335$ nm), $\rho_s$ is the number density of carbon atoms in graphite (114 nm$^{-3}$), and $\sigma_{sf}$ and $\varepsilon_{sf}/k$ are the solid-fluid Lennard-Jones parameters (0.3605 nm and 64.4 K, respectively [17]). Note that this potential is a function only of the distance $z$ from the wall, and does not include

TABLE I. Summary of results for simulations at temperature $kT/\varepsilon = 2.0$, pore size $H/\sigma = 2.5$, and width ($y$ direction) $W/\sigma = 10$, for diffusely reflecting walls.

| Run | $\exp(\beta\mu)\Lambda^{-3}$ (sink) | $\rho\sigma^3$ (sink) | $\exp(\beta\mu)\Lambda^{-3}$ (source) | $\rho\sigma^3$ (source) | $\ell/\sigma$ | $J\sigma^3(m/\varepsilon)^{1/2}$ |
|---|---|---|---|---|---|---|
| 1 | 0.0020 | 0.1117 | 0.0021 | 0.1162 | 13.3 | $3.0 \times 10^{-4}$ |
| 2 | 0.0020 | 0.1117 | 0.0035 | 0.1593 | 13.3 | $3.2 \times 10^{-3}$ |
| 3 | 0.0020 | 0.1117 | 0.0035 | 0.1593 | 20.0 | $2.3 \times 10^{-3}$ |
| 4 | 0.02 | 0.2845 | 0.03 | 0.3076 | 13.3 | $3.9 \times 10^{-3}$ |
| 5 | 0.02 | 0.2845 | 0.03 | 0.3076 | 20.0 | $2.4 \times 10^{-3}$ |

any graphitic surface structure. The total adsorbate-pore potential is the sum of the interactions from both walls.

The simulations contained between 150 and 400 particles and were run for about 4 ns. Each run took approximately 170 h of CPU time on a Silicon Graphics r4000 workstation in the Department of Chemistry at Imperial College.

The results from the simulations described in this work were compared with results from EMD calculations for the same model, given in Ref. [17]. Simulations using a specular wall condition gave fluxes about one and a half orders of magnitude higher than would be predicted from the transport diffusivities. Difficulty was experienced in obtaining accurately converged fluxes with this wall condition. In the remainder of this Letter we report results for the diffuse wall condition and a pore of width $H/\sigma = 2.5$ at a temperature of $kT/\varepsilon = 2.0$. Details of the runs are summarized in Table I. Figure 2 shows a plot of pore concentration versus distance along the pore (in the flow direction) for run 2. The volume used in the calculation of concentration uses the carbon atom to carbon atom distance, $H$, between the two opposite pore walls which includes a certain amount of dead space due to the physical size of the wall atoms. The concentrations in the control regions are approximately constant, except at the ends of the simulation box where the concentration falls to zero as the particles disappear into oblivion.

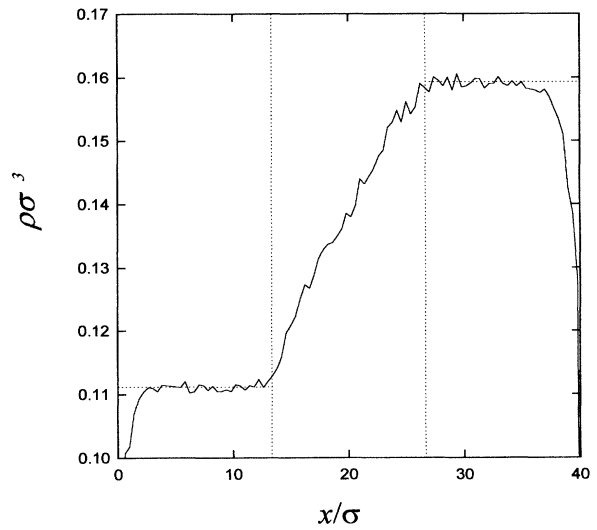


FIG. 2. Density profile along the flow direction for a pore of width $H/\sigma = 2.5$, temperature $kT/\varepsilon = 2.0$. Length of flow region: $l/\sigma = 13.3$. Source region chemical potential: $\exp(\beta\mu)\Lambda^{-3} = 0.0035$. Sink region chemical potential: $\exp(\beta\mu)\Lambda^{-3} = 0.0020$. The vertical and horizontal broken lines indicate the boundaries of the flow region, and the mean source and sink densities, respectively.

Figure 3 shows the $z$ velocity averaged over the flow region (bars), and the average pore density, both as functions of distance from the pore wall in run 2. The velocity profile shows an approximately parabolic profile with no evidence of significant slip. This compares with the work of Hannon, Lie, and Clementi [3] who observed slip in a simulation using diffuse reflection and hard walls. The attribution of slip in their simulation to the "absence of any attractive force between the walls and the molecules to offset any attractive intermolecular forces" is consistent with this work since our simulation contains an attractive wall-adsorbate interaction.

Figure 4 shows flux plotted against average gradient for the five runs in Table I. The points (circles) from runs 1, 2, and 3 all fall on a straight line passing through the

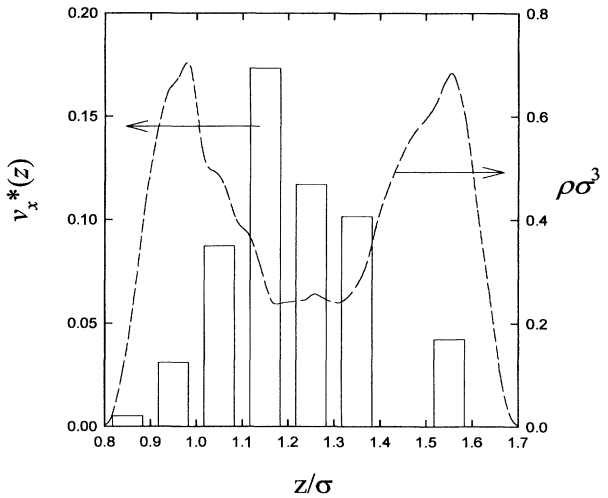


FIG. 3. Average density (---) and velocity [$v^* = v(m/\varepsilon)^{1/2}$] profile (bars) in the flow region as a function of distance from the pore walls. Same conditions as Fig. 2.

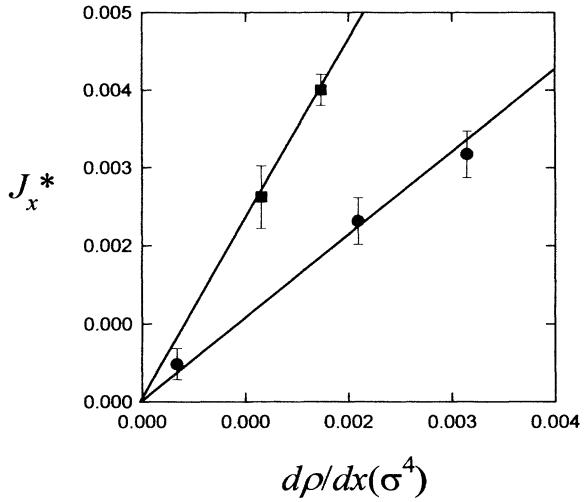


FIG. 4. Flux $[J^* = J\sigma^3(m/\varepsilon)^{1/2}]$ vs concentration gradient for a pore of width $H/\sigma = 2.5$, at temperature $kT/\varepsilon = 2.0$. Average pore density: $\rho\sigma^3 \approx 0.136$ (●), $\rho\sigma^3 \approx 0.296$ (■).

origin. Similarly the points corresponding to a higher pore density (squares) from runs 4 and 5 fall on a different straight line passing through the origin. Fick's law [8] therefore appears to be obeyed, within the errors of the flux calculations. Measurement of the gradients give diffusion coefficients in reduced units ($Dm^{1/2}\varepsilon^{-1/2}\sigma^{-1}$) of 1.06 and 2.27 corresponding to the lower and higher pore densities, respectively. By comparison the EMD results for transport diffusion from Ref. [17] ($q\nu$) give reduced transport diffusivities of 0.48 (corresponding to $\rho\sigma^3 = 0.135$) and 0.63 (corresponding to $\rho\sigma^3 = 0.29$). The ratio of the NEMD coefficients to the EMD coefficients are 2.2 at density $\rho\sigma^3 = 0.135$ and 3.6 at density $\rho\sigma^3 = 0.29$. This is in good qualitative agreement with Maginn, Bell, and Theodorou [9] who observed, for methane in silicalite at 300 K, that the ratio of NEMD diffusivity to EMD transport diffusivity was always greater than unity and increased with pore filling. The differences are attributed to the increasing importance of cooperative (viscous) effects.

The chemical potential gradients simulated here are considerably higher than anything likely to be encountered in an experimental situation. For example, run 2 corresponds to a pressure drop of approximately 35 atm across a 50 Å length of pore; nevertheless a linear relationship between flux and gradient is observed. The method does not intrinsically require linearity, and it was not clear *a priori* that it would be found; the method has obvious potential in determining nonlinear transport coefficients under very high gradients [10]. Having demonstrated the viability of this NEMD scheme, we plan to study nonlinear transport behavior in future work as well as exploring the effects of temperature and pore size.

This work was funded by the European Union and British Petroleum plc under BRITE EURAM Contract No. BREU-CT92-0568.

*Authors to whom correspondence should be addressed.
*

[1] S. R. De Groot and P. Mazur, *Nonequilibrium Thermodynamics* (North-Holland, Amsterdam, 1962).
[2] E. A. Mason and L. A. Viehland, J. Chem. Phys. **68**, 3562 (1978).
[3] L. Hannon, G. C. Lie, and E. Clementi, Phys. Lett. A **119**, 174 (1986).
[4] J. Koplik, J. R. Banavar, and J. F. Willemsen, Phys. Fluids A **1**, 781 (1989).
[5] U. Heinbuch and J. Fischer, Phys. Rev. A **40**, 1144 (1989); G. Mo and F. Rosenberger, Phys. Rev. A **42**, 4688 (1990); D. K. Bhattacharya and G. C. Lie, Phys. Rev. A **43**, 761 (1991); S. Sokolowski, Phys. Rev. A **44**, 3732 (1991).
[6] I. Bitsanis, J. J. Magda, M. Tirrel, and H. T. Davis, J. Chem. Phys. **87**, 1733 (1987); L. A. Pozhar and K. E. Gubbins, J. Chem. Phys. **99**, 8970 (1993).
[7] M. P. Allen and D. J. Tildesley, *Computer Simulations of Liquids* (Oxford University Press, Oxford, 1987).
[8] J. Kärger and D. M. Ruthven, *Diffusion in Zeolites and Other Microporous Solids* (Wiley, New York, 1992).
[9] E. J. Maginn, A. T. Bell, and D. N. Theodorou, J. Phys. Chem. **97**, 4173 (1993).
[10] D. J. Evans and G. P. Morris, *Statistical Mechanics of Non-Equilibrium Liquids* (Academic, San Diego, 1990).
[11] M. Sun and C. Ebner, Phys. Rev. A **46**, 4813 (1992); Phys. Rev. Lett. **69**, 3491 (1992).
[12] M. M. Cielinski, M.S. thesis, University of Maine, Orono, 1985; M. M. Cielinski and N. Quirke (unpublished).
[13] T. Caginn and B. M. Pettit, Mol. Simul. **6**, 5 (1991).
[14] A. Popadoulou, E. D. Becker, M. Lupkowski, and F. van Swol, J. Chem. Phys. **98**, 4897 (1993).
[15] G. S. Heffelfinger and F. van Swol, J. Chem. Phys. **100**, 7548 (1994).
[16] D. Brown and J. H. R. Clarke, Mol. Phys. **51**, 1243 (1984).
[17] R. F. Cracknell, D. Nicholson, and K. E. Gubbins, J. Chem. Soc. Faraday Trans. (to be published).
[18] W. A. Steele, *The Interaction of Gases with Solid Surfaces* (Pergamon, Oxford, 1974).